

TECHNICAL REPORT NO. 417

SOME INVESTIGATIONS WITH LASER BEAMS

ON AN LLA RETINA

BY

AMITAVA BISWAS

AUGUST 1994

**COMPUTER SCIENCE DEPARTMENT
INDIANA UNIVERSITY**

BLOOMINGTON, INDIANA 47405-4101

**SOME INVESTIGATIONS WITH LASER BEAMS
ON AN LLA RETINA**

Amitava Biswas

**Submitted to the faculty of the University Graduate School
in partial fulfillment of
the requirements for the degree
Master of Science
in the Department of Computer Science
Indiana University**

August, 1994

Accepted by the Graduate Faculty, Indiana University, in partial fulfillment
of the requirements for the degree of Master of Science.

Steven Johnson, Ph.D., Chairman, Computer Sc. Dept.

M.S.Committee:

Jonathan Wayne Mills, Ph.D. Principal Advisor.

Edward Robertson, Ph.D.

Steven M. Barlow, Ph.D.

August 10, 1994

Acknowledgements

I wish to express my gratitude to Professor Jonathan Mills for advice, motivation and encouragement for this work. His never ending series of innovative ideas kept my project running. Professor Steven Johnson provided all available support. Professor Edward Robertson inspired me by his warm attitude. Professor Steven Barlow helped me out of the difficult moments. All of them made valuable suggestions that improved the presentation of this thesis.

Andrew Heininger did the initial research and development on the LLA Retina with Professor Mills and started the basic investigation on these devices [7]. Bob Montante never refused any request for help. Jason Almeter used to answer all my questions heartily. Shankar Swamy explained to me many tricks of the trade. Ratnakar Amaravadi was a friend in need.

My daughter Asima and wife Archana shared most of the typing work for this thesis.

Amitava Biswas

Abstract

The HLA Retina combines Lukasiewicz logic arrays (HLAs) with photo-sensor clusters to work as a fuzzy edge detection mechanism and several other applications. In this presentation we have explored various approaches to excite and evaluate the device with several types of light sources including visible and infra-red laser beams. Based on the detailed studies on the device, one particular configuration was designed and tested to perform as an edge detector.

Contents

Acknowledgements	iii
Abstract	iv
List of Tables	vii
List of Figures	viii
1. Introduction	1
1.1 Background	1
1.2 Purpose	1
1.3 Overview	2
2. Instrumentation	3
2.1 Basic Scheme	3
2.2 ADC Card	4
2.3 Fluke-97 Scope	4
3 Laser Sources	6
3.1 Laser-A	6
3.2 Laser-B	7
3.3 Laser-C	7
3.4 Laser-D	8
4. Static Characteristics	9
4.1 Setup	9
4.2 Results	10
5. Dynamic Characteristics	15
5.1 Effect of Intensity	15
5.2 Square-Wave Response	16

6. Scanned Behavior	22
6.1 Setup	22
6.2 Results	22
7. Array Behavior	25
7.1 Setup	25
7.2 Results	25
8. Temperature Effect	27
9. Beam Pattern	29
9.1 Setup	29
9.2 Results	30
10. Edge Detection	33
10.1 Circuit Details	34
10.2 Theory of Operation	35
11. Conclusion	38
References	39
A. PC-Eye1 Cell Arrangement	41
B. Pinout Details of LLA9a	42
C. Data Acquisition Session	43
D. Units and Conversions	45
E. Photographs of PC-Eye1	46

List of Tables

C.1 Typical Data Acquisition from the ADC card	43
C.2 Typical Data Transfer from Fluke97 scope	43
C.3 A Sample Data Dump from Fluke97 scope	44
D.1 Units of Luminous Flux Density at a Surface	45
D.2 Conversion of Illuminance Units	45
D.3 Typical Light Sources	45

List of Figures

2.1 Experimental Setup	5
4.1: PC-Eye1 Characteristics at Pin 1	11
4.2: PC-Eye1 Characteristics at Pin 6	12
4.3: PC-Eye1 Characteristics at Pin 11	13
4.4: PC-Eye1 Characteristics at Pin 20	14
5.1: PC-Eye1 Dynamic Response at Full Laser Drive	17
5.2: PC-Eye1 Dynamic Response at Medium Laser Drive	18
5.3: PC-Eye1 Dynamic Response at Low Laser Drive	19
5.4: PC-Eye1 Response with Square Wave Laser Drive	
20	
5.5. Laser Drive Rise and Fall times	21
6.1. Two Cells Scanned by Laser Beam	23
6.2. Response with Bar Code Scanner	24
7.1. PC-Eye1 Array Response	26
8.1. Forward Drop of Pin 1 at 75 micro amps	28
9.1. Beam Spread when focused at 500 microns	
31	
9.2 Beam Spread when focused at 3000 microns	
31	
9.3. Same as Fig.9.2 but a little out of focus	32
9.4. Same as Fig.9.2 but more out of focus	
32	

10.1. Logic Tree of Edge Detection using LL9a	
36	
10.2. Edge Detection Behavior	37
E.1. Photograph of PC-Eye1 on Test Board	46
E.2. Photograph of Fluke-97 Display	46

1

Introduction

1.1: Background

The author began this investigation during the fall of 1992 when Mills and Heining developed a new VLSI chip named PC-Eye1, also called the Retina chip. The primary goal was to achieve good edge detection properties by combining this photo sensor with LLAs, developed by Mills [1]. This combination is called an LLA Retina. The initial experiments indicated very good potential for such a device [7]. During the early stages, the edge was created by projecting a shadow directly on the photo cells. As the shadow had a penumbra, diffused semi-dark regions spread over a large area and the edge transition area of a typical shadow was more than the size of the photocell array. This problem was resolved by using a tiny lens to project a sharper image on the Retina chip [7].

1.2: Purpose

The investigation described in this thesis extends the above work by detailed experiments to evaluate static and dynamic characteristics of the Retina chip, more precise measurements using laser beams, and design and testing of an edge detection algorithm using the LLA-Retina combination.

1.3: Overview

Here is a brief overview of this document. Firstly, we have presented some details about the instrumentation strategy adopted for the investigation. Then some details about the laser sources are provided. This is followed by reports on measurements of static and dynamic characteristics of some selected photocells of the Retina chip. These characteristics are useful to design an application circuit with the Retina chip. Other tests performed on the Retina chip include response of the photocells under a scanning beam and group response of an array of photocells of the chip. These measurements show suitability of the Retina chip for applications such as edge detection. The beam pattern of one of the laser sources was measured in detail and reported here. This measurement indicates the precision level available with a typical inexpensive laser setup. An edge detection circuit was constructed and tested based on the experience gained over the previous results. Some details about the pinout connections of the chips, sample data acquisition programs, typical units and conversions etc., are presented in the appendix.

2

Instrumentation

2.1: Basic Scheme

The basic scheme of instrumentation used for this investigation is shown in Figure 2.1. At the center of the figure, is the Retina chip under test. A beam of light was projected on the chip from either a tungsten bulb or a laser source. For measurement of static characteristics, the tungsten bulb was used to provide uniformly distributed light. For measurement of dynamic characteristics a pulsed laser beam was used. The sources of laser are described in section 3. The Retina chip was mounted on a microscope translation stage for high precision positioning. Some of the cells in the chip were activated by pull-up resistors to a dc supply. The voltage drop across the resistors were measured by a Fluke-97 digital oscilloscope. Details of which cells of the chip were tested are given under specific experiments later. For some experiments the data was captured by an ADC card. The received data was stored and processed in a PC. For the edge detection experiment, the output of some of the photocells were fed to a LL9a chip. The details of this experiment is given in section 10. A photograph of the Retina chip on a test board is shown in Figure E.1.

2.2: ADC card

Multichannel measurements were performed using an ADC card installed inside an IBM compatible PC. The card was accessed by instructions in high level language. A sample data acquisition program is given in table C.1. This card is useful for low speed measurements only. It has a 12 bit resolution. It was used in experiments where output from several photocells are to be grabbed simultaneously. It has no restriction on the number samples to be grabbed in a session compared to the Fluke-97 digital scope described in the following section.

2.3: Fluke-97 Scope

For high speed measurement, a Fluke97 digital scope was used. Its upper speed limit of 50 MHz was adequate for our purpose, because it could show very good details in time scale. This was useful to digitize pulse rise and fall patterns, shown later. However the details in amplitude was limited to 8 bits. The resulting waveforms showed some quantization jitter. Another limitation of this instrument was that it could grab only 512 or 256 samples at a time. An optical interface for the scope was developed by the author to transfer data arrays from the scope memory to an IBM compatible PC. The interface was accessed by instructions in high level language. A sample data acquisition program is given in table C.2. The result of a data dump session is shown in table C.3. Every dump is preceded by a standard header. In the example shown in table C.3, the header says that the data originated from channel A. The header also records that the vertical resolution was 2 millivolts per dot. The horizontal resolution was 80 nanoseconds per dot and the probe zero was mapped to the 56th dot on the Y axis in this particular

measurement. A photograph of a typical display on the digital oscilloscope is shown in Figure E.2.

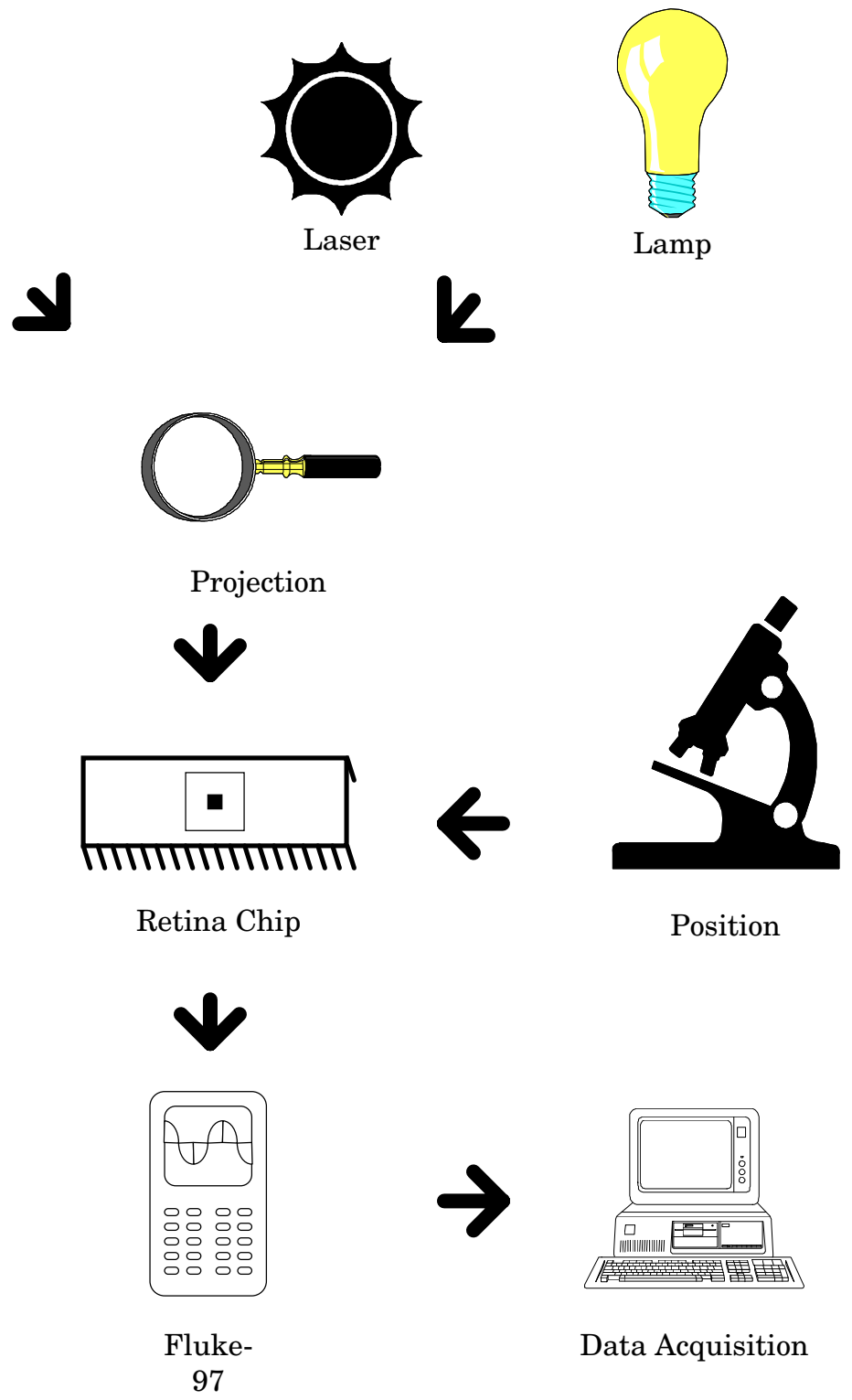


Figure 2.1: Experimental Setup

3

Laser Sources

Four sources of laser beams were used by the author. All of them were low power devices, each giving about 1 milliwatt output. A brief description of these devices is given below. Depending on several factors, such as whether the output beam is stationary or scanning, whether the beam is pulsed etc., a particular source was chosen for a particular experiment. These sources will be referred later as A,B,C and D.

3.1: Laser-A

This is a conventional Helium-Neon laser source that operates at 12 volts, drawing about 1 ampere. It has a self contained high voltage converter to generate 1250 volts at 5 milliamperes for the laser tube. The advantage of this beam is that it gives a very stable, sharp and visible laser beam. It is useful where dynamic pulsing or scanning is not necessary. Its disadvantages are that the beam can not be modulated by external electrical signals. Neither is there any simple way to scan the beam at uniform rates. This beam was used for initial setup and testing purpose only.

3.2: Laser-B

The second laser beam source is a typical UPC scanner. This has a solid state laser diode that emits a red beam. It operates from an external 12 volt power supply, drawing about 0.5 amperes. The beam is automatically scanned by a vibrating mirror. This device is suitable where uniform scanning rate is useful. However the device has no provision to give a stationary beam.

3.3: Laser-C

The third laser beam source was constructed out of a music CD player. The servo drive and circuitry of the player were partially modified to gain access to the main functions of the moving head. Three external potentiometers and three toggle switches were added to allow the operator to adjust focus, side shift and scanning rates. The advantage of this setup is that very convenient focusing is achieved by one of the 10 turn potentiometers. Another potentiometer controls the amount of lateral shift of the laser beam. The third potentiometer adjusts the scanning rate of the laser beam. One toggle switch was added to turn the beam on and off. This was interconnected to a beeper and an LED to alert the operator of the presence of the laser radiation. Another toggle switch was added to control the direction of offset of the beam. The third toggle switch controlled the scanning direction of the moving head. This device operates directly from 120 volt mains, having its own power supply circuit. The beam is infra-red and therefore it is not

suitable where visible beam is needed. There is no provision to pulse the beam.

3.4: Laser-D

The fourth laser beam source used in this investigation was a solid state infrared laser diode directly pulsed by a TTL circuit. It was designed and built by the author with several useful features. The unit is very compact, about 6"x3"x2". It has its own 7.5 volt storage battery to ensure very stable and noise-free power to the electronics. It has an adjustable projection lens to focus the beam. But the beam is not visible. Therefore four high intensity red LED's were fixed around the laser diode. The LED's projected four bright spots and made it easy to estimate the laser beam position, positioned at their center. Two of the four LED's are slightly closer to the projection lens than the laser diode, whereas the other two are fixed slightly away from the lens. This arrangement helped estimate the exact image position of the laser diode. The amount of axial adjustment necessary is indicated by appearance of relative sharpness of the LED images. The laser diode was pulsed at about 1 megahertz by a built-in pulse-generator and driver. The rise time of the drive pulse is about 20 nanoseconds and the fall time is about 25 nanoseconds, by actual measurement. To notify nearby people that the laser beam was in operation, and also to remind the experimenter of the constant current drain, the system gives a short beep every two minutes.

4

Static Characteristics

4.1: Setup

To assess correct operating conditions, detailed static characteristics of PC-Eye1 were evaluated. Several 52 watt tungsten bulbs were used to create the desired illumination level. The average light output of a 52 watt tungsten bulb is 700 lumens. This arrangement provided enough illumination to drive the photo-transistors. Four levels of illumination level were used at 8, 20, 100 and 200 foot candles. 8 foot-candles of illumination level is quite low, whereas 200 foot-candles is a strong level of illumination, comparable to a dark room and a lighted hallway, respectively. The photo sensitive cells in the Retina chip are divided into four groups, according to size. For this experiment, one cell from each group was chosen to reduce the number of measurements. The four cells had external connections at pins 1, 6, 11 and 20. Their positions and other details are shown in appendix A. For a particular level of illumination, each of these four cells was tested for amount of flowing current when a particular voltage was applied. To prevent damage to the cell under test, a series resistor of 10k ohms was used instead of direct connection to the voltage source.

4.2: Results

The static characteristics are plotted in Figures 4.1 through 4.4. The transistor characteristics are similar to those photo cells. Each figure gives voltage-current characteristics of one cell at four levels of illumination. The curves are marked with squares, circles, triangles and diamonds for illumination levels of 200, 100, 20 and 8 foot-candles respectively. The characteristics reveal that the current value at a particular voltage for a particular cell is almost directly proportional to the illumination level. From these characteristics it is possible to estimate the value of a suitable load resistor for a particular group of cells at a particular range of illumination. If the resistor is too small then the voltage drop would be too small, if the resistor is too large then the photocell gets saturated easily. The four figures also show that the single cells pass more current relative to the doublet cells.

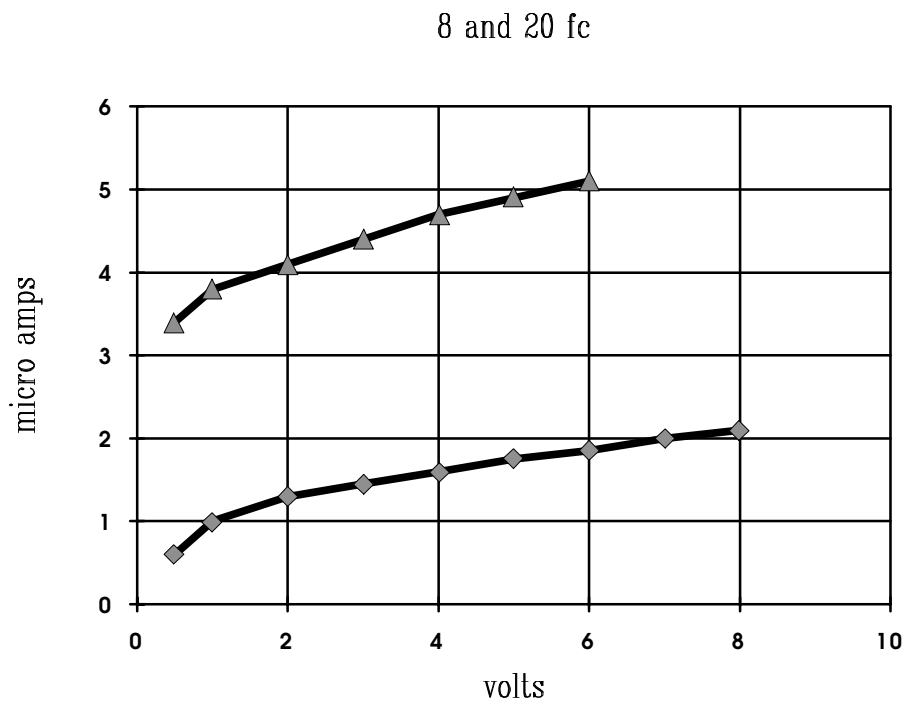
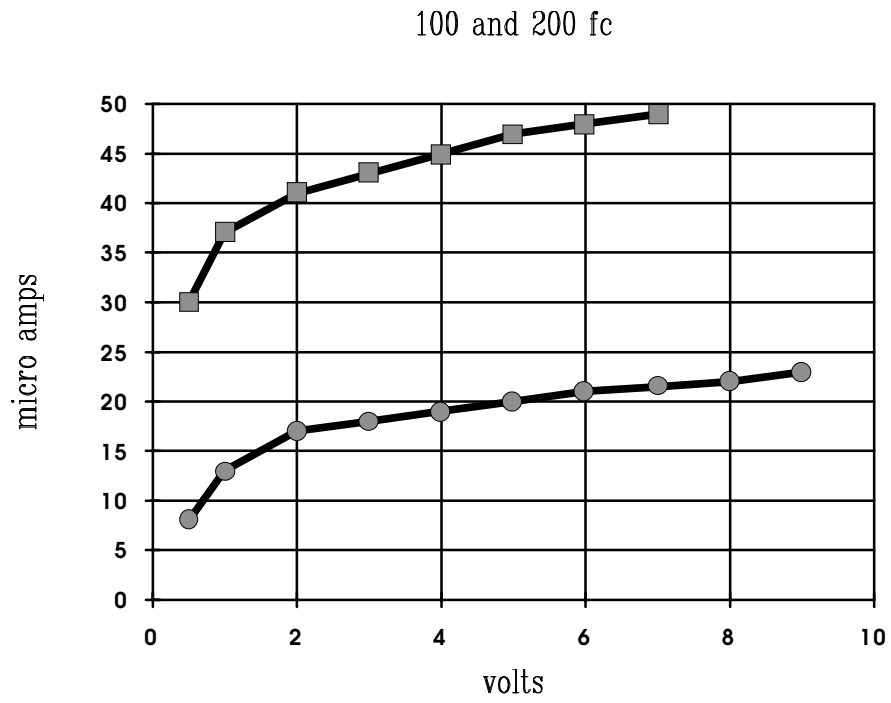


Figure 4.1: Typical Characteristics of PC-Eye1 at Pin 1

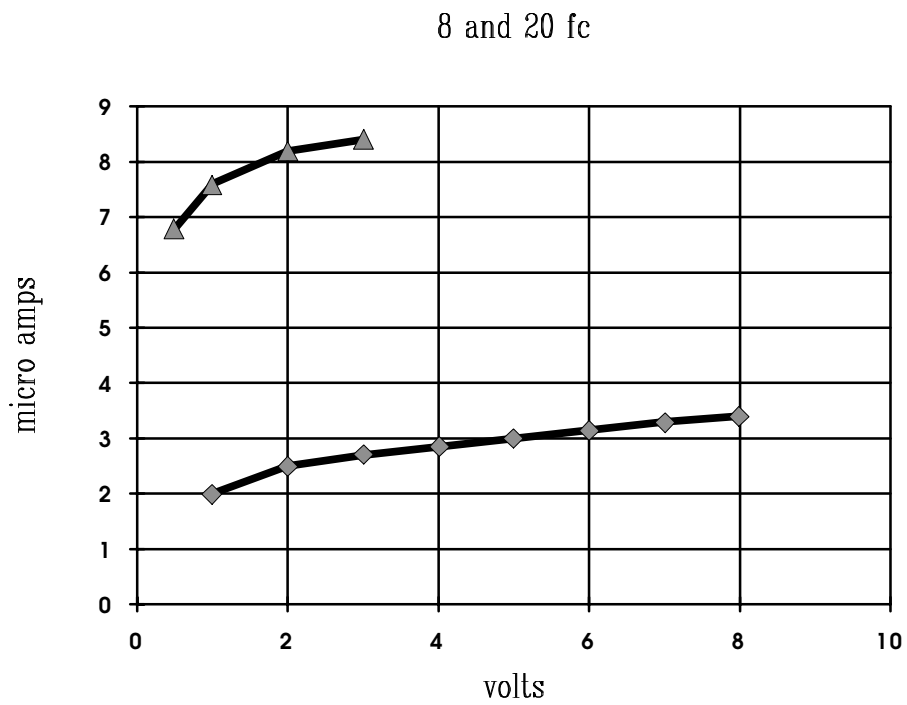
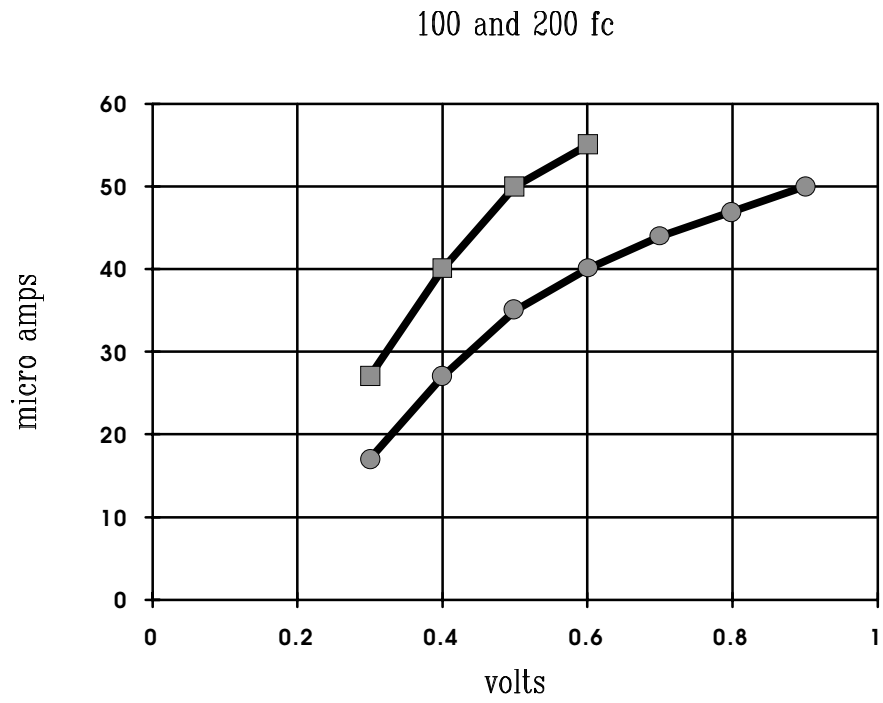


Figure 4.2: Typical Characteristics of PC-Eye1 at Pin 6

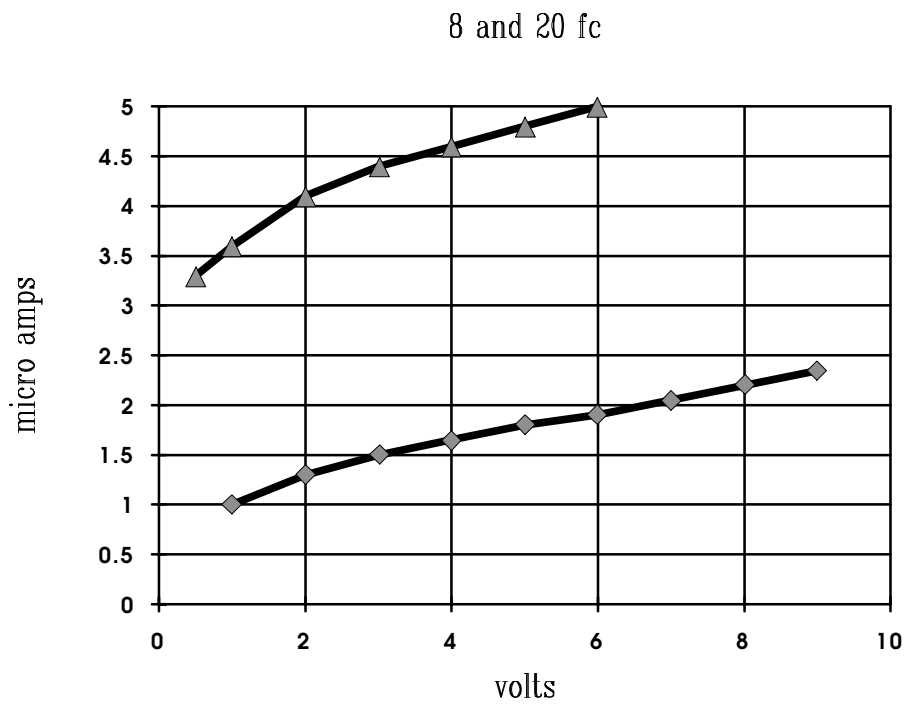
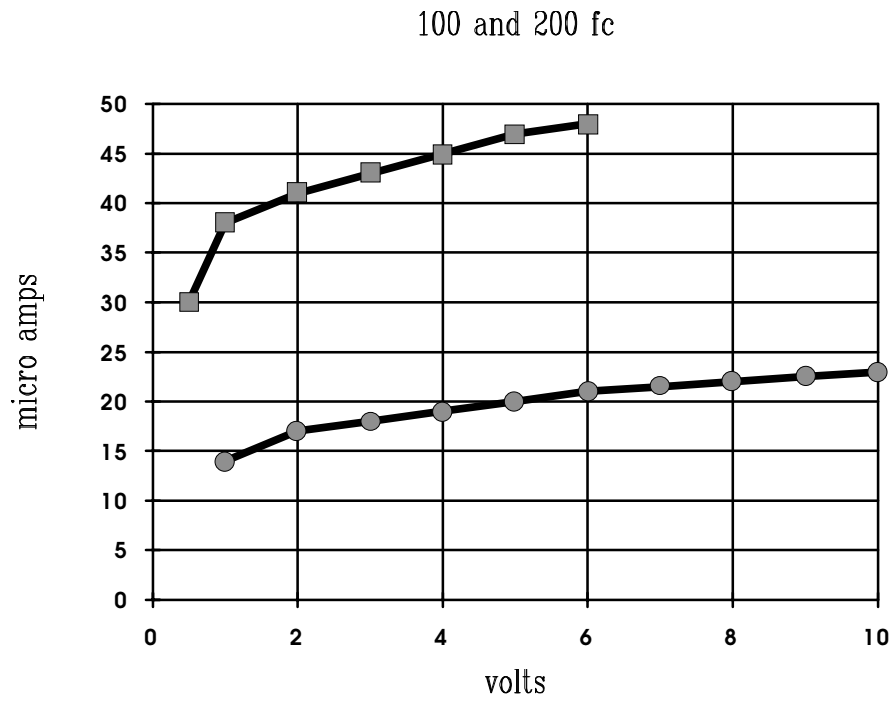
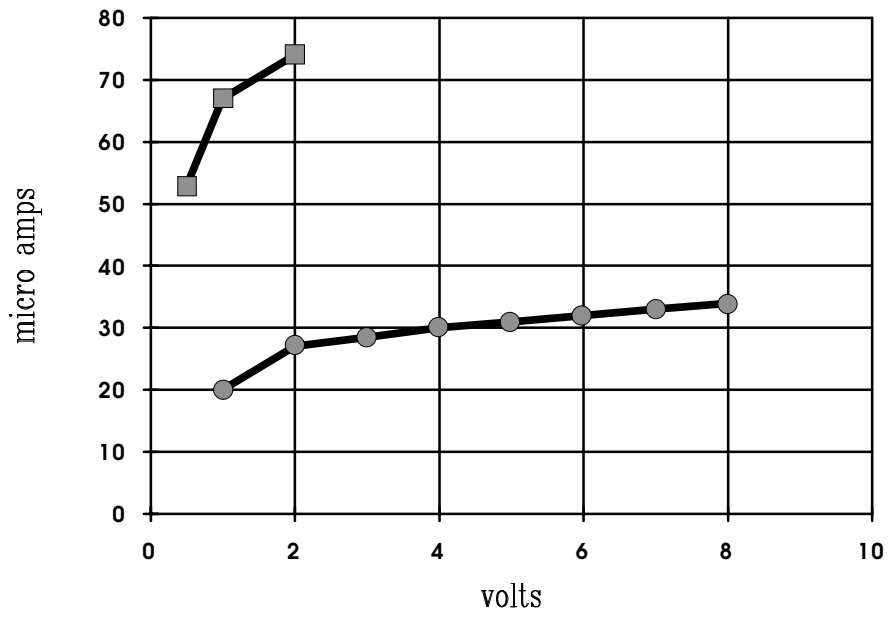


Figure 4.3: Typical Characteristics of PC-Eye1 at Pin 11

100 and 200 fc



8 and 20 fc

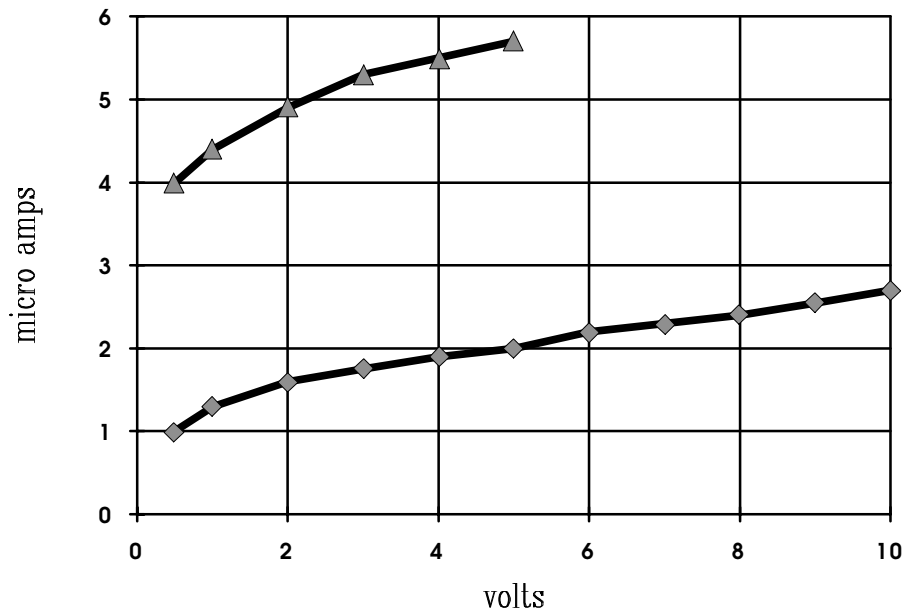


Figure 4.4: Typical Characteristics of PC-Eye1 at Pin 20

Dynamic Characteristics

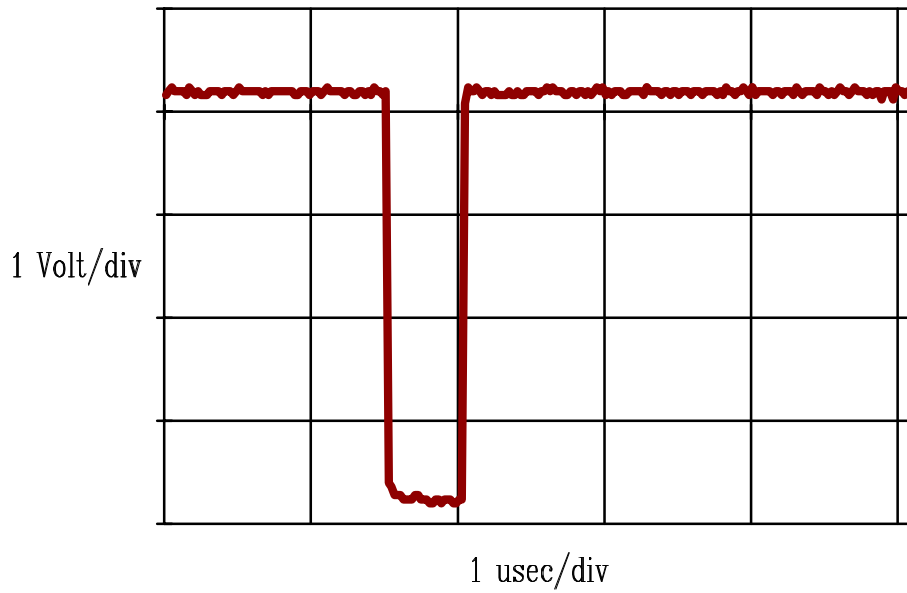
5.1: Effect of Intensity

To assess the transient behavior of the retina chip, several experiments were conducted. The first set of experiments was conducted in collaboration with a visiting team from the office of Naval Research during September, 1993. They provided the laser source for this experiment. This source had provision to pulse the beam at varying intensity. The photo-cell chosen for this experiment had external connection at pin 21. Appendix A shows the location and other details of this cell. It was connected to 5 volts supply with a 10k ohms pull-up resistor. The laser source was positioned at about 500 millimeters from the chip. The laser beam was infra-red and therefore invisible. A special phosphorescent paper was used to find the beam spot. The results are shown in Figures 5.1, 5.2 and 5.3. In each figure, the upper graph shows the drive to the laser module and the lower graph shows the corresponding response at a photo cell of the Retina chip. In the Figure 5.1 the laser drive is set at the high intensity position. In this case, the response has sharp fall but the rise has large delay. In Figure 5.3 the laser drive is set at the low intensity position. In this case the response has slower fall time. The rise time has less delay but the photocell output did not fall below 1 volt in this case. The Figure 5.2 shows intermediate conditions with the laser drive was set at medium intensity position.

5.2: Square-wave Response

Another set of transient measurements was taken using the laser source D described in section 3.4. The chip was kept at a distance of about 200 millimeters from the laser source. The photo cell chosen for this experiment had external connection at pin 21. It was connected to 5 volts supply with a 1k ohms pull-up resistor. The voltage drop across the load resistor was monitored and grabbed by a Fluke 97 digital oscilloscope, similar to the experiment in section 5.1. The rise and fall time of the laser drive are shown in Figure 5.5. In the upper trace of Figure 5.4, the laser diode is given square wave pulses. The Retina response given in the lower trace appears sinusoidal due to attenuation of higher frequencies. Some background noise appears in the waveforms, primarily due to the quantization effect of the 8 bit analog to digital converter. This experiment shows that the chip can handle signals upto 1 MHz.

Laser Drive



PC-Eye1 Response

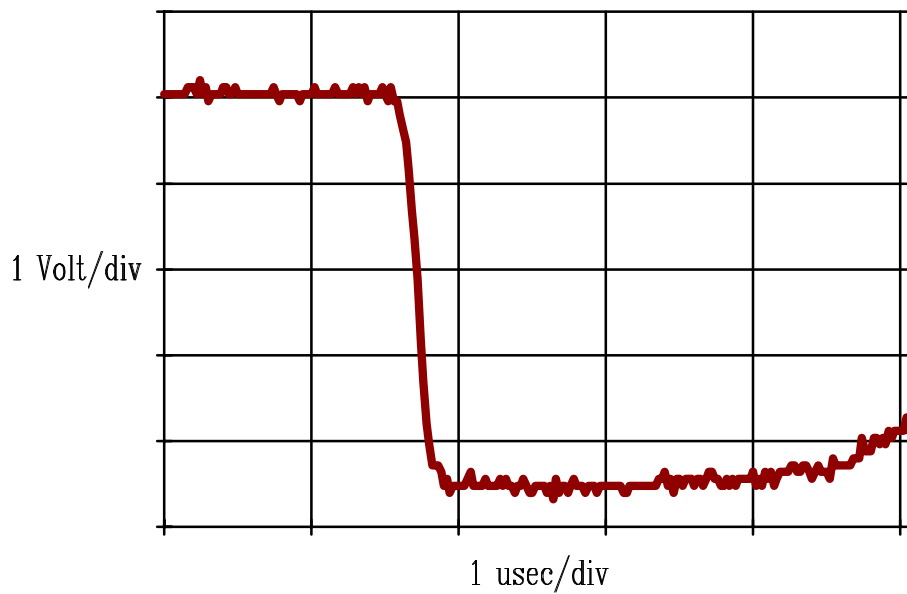
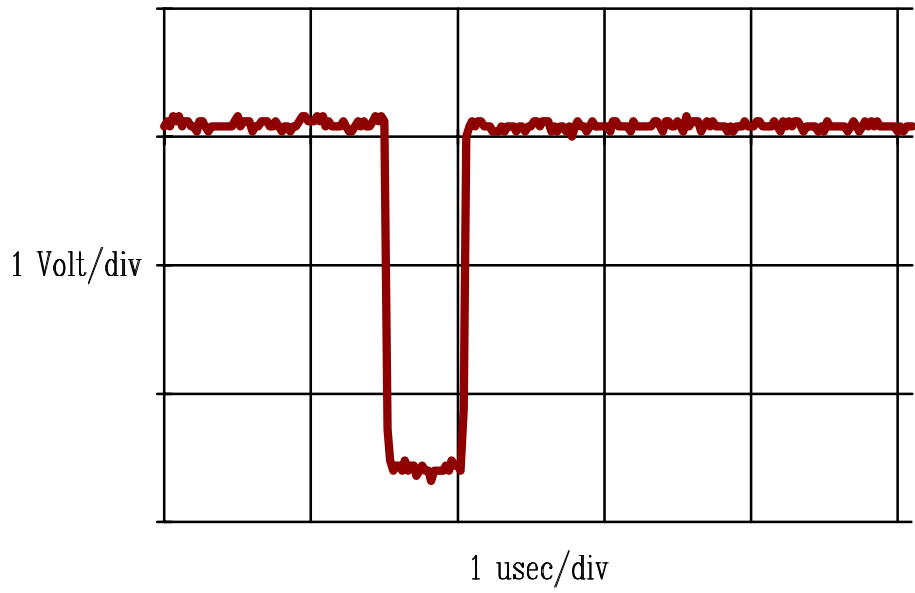


Figure 5.1: Typical PC-Eye1 Response at High Laser Drive

Laser Drive



PC-Eye1 Response

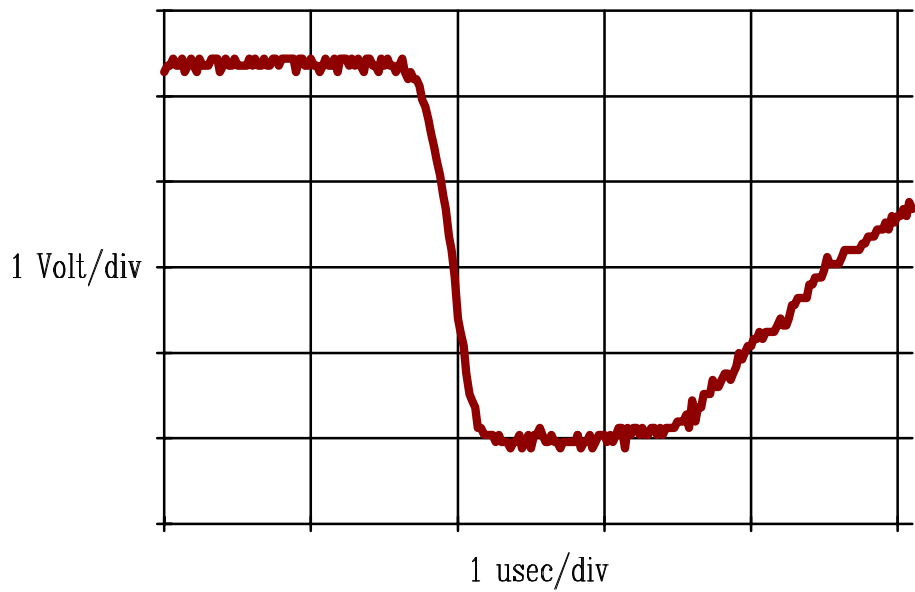
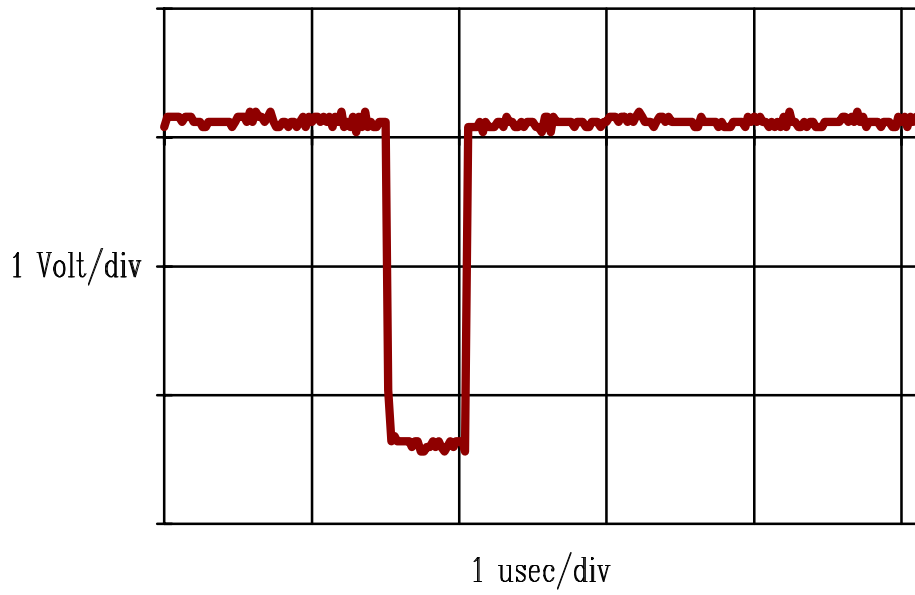


Figure 5.2: PC-Eye1 Response at Medium Laser Drive

Laser Drive



PC-Eye1 Response

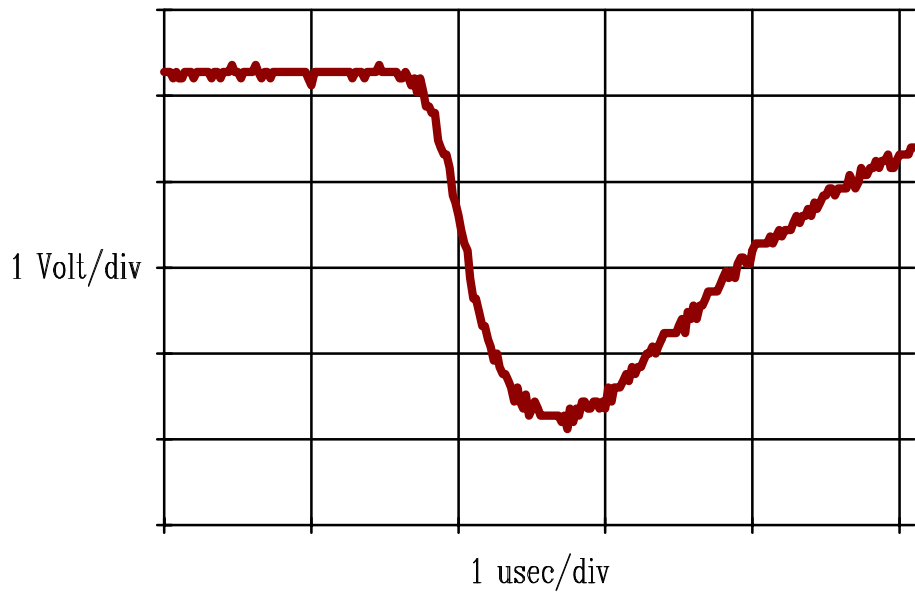
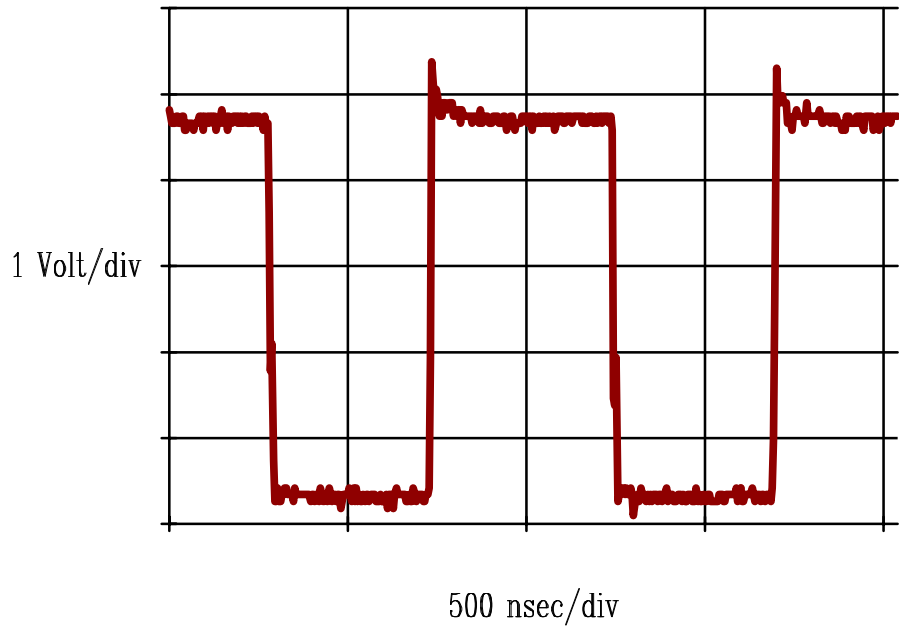


Figure 5.3: PC-Eye1 Response at Low Laser Drive

Laser Drive



PC-Eye1 Response

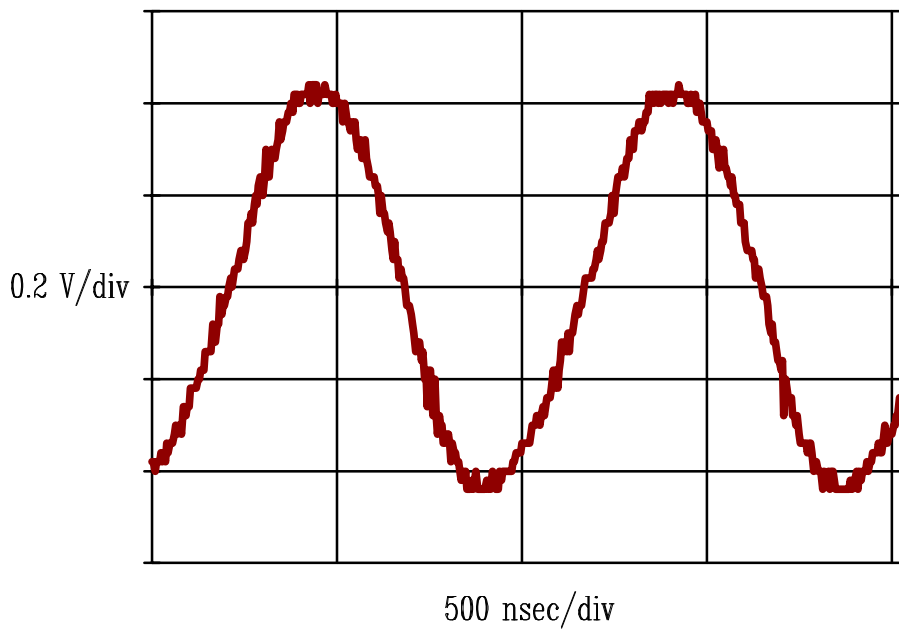
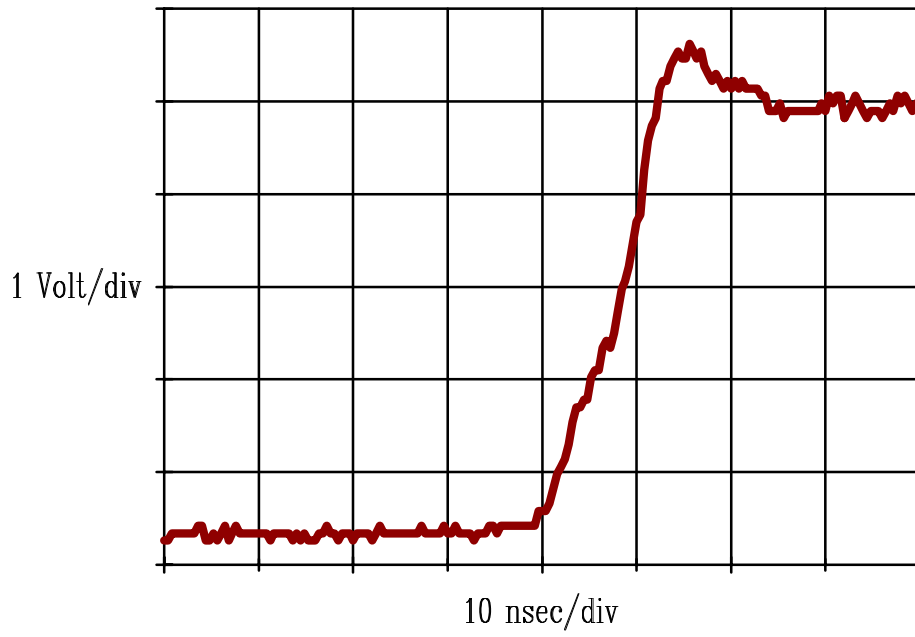


Figure 5.4: PC-Eye1 Response with Square Wave Laser Drive

Laser Drive Rise Time



Laser Drive Fall Time

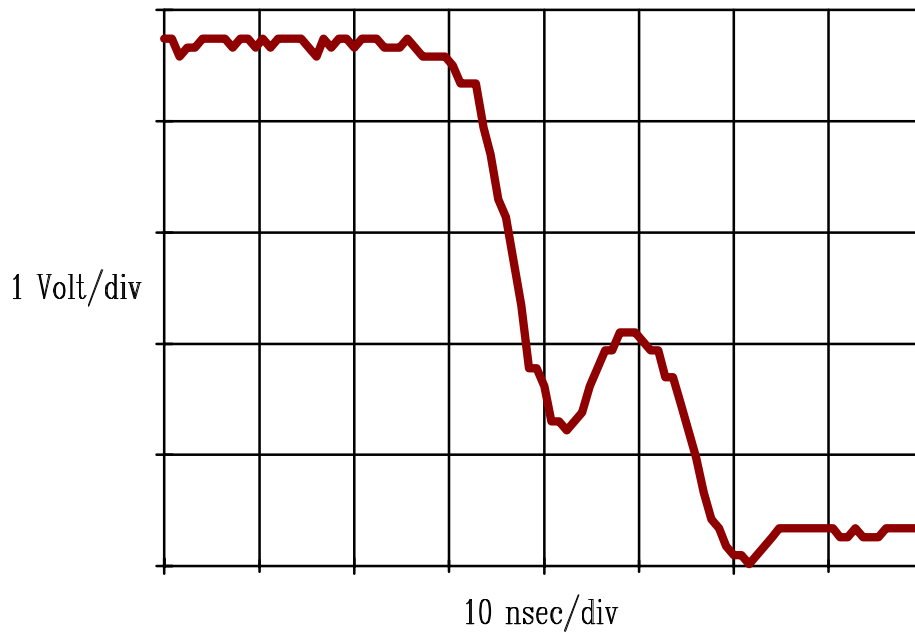


Figure 5.5: Laser Drive Rise and Fall Times

6

Scanned Behavior

6.1: Setup

For dynamic detection of moving edges the Retina chip must detect changes in the spatial orientation of light falling on the sensors, in addition to its ability to detect changes in light intensity levels. This property was tested by projecting a scanned ray of laser light from the source-B, described in section 3.2. Two cells of the chip were monitored simultaneously by a Fluke-97 digital oscilloscope. These two cells had external connection at pins 21 and 26. The supply voltage was 5 volts and the pull-up resistors were 10k ohms for both cells.

6.2: Results

In Figure 6.1, the upper trace shows the response at pin 21 and the lower trace shows the response at pin 26. The relative shift in the response pulse is due to the spatial distance between the corresponding cells and the time to cover this distance by the moving spot of light. If the spot were not very well defined then the two pulses would have appeared to be merged into one. Figure 6.2 shows the rise and fall time of the pulse at pin 21 in greater detail. It is noted here that the rate of rise is much slower than the rate of fall. This is because during fall time the photo cell conducts and shortens the system response, but during rise time the photo cell is off and increases the system response time. It is expected that the response might be faster with

smaller load resistor but at the expense of reduced overall output voltage swing.

Pin 21



Pin 26

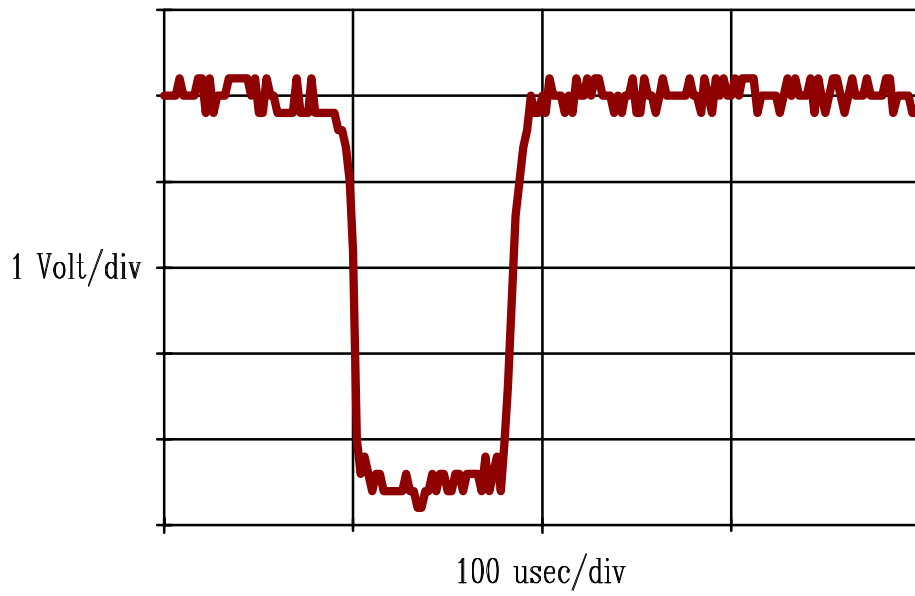
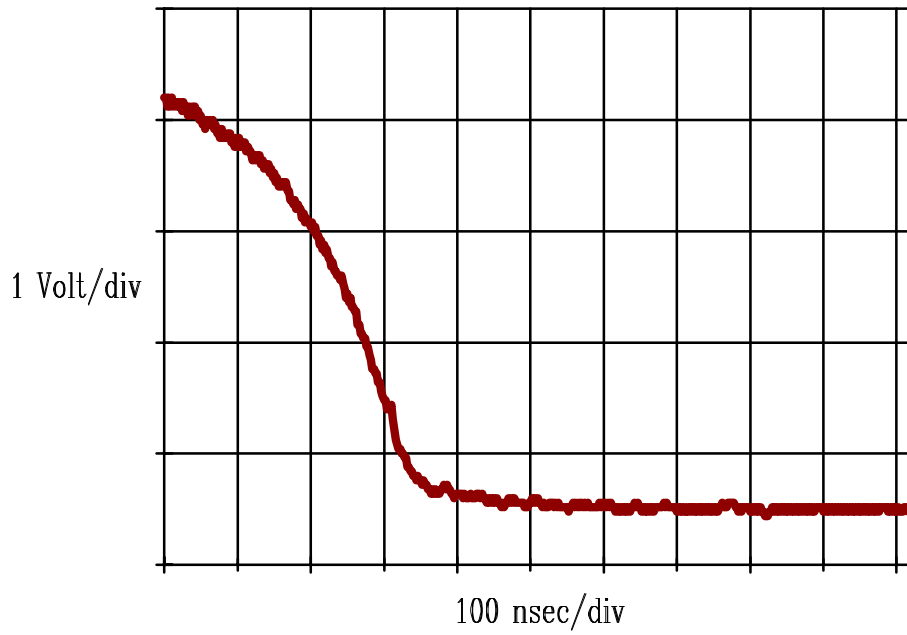


Figure 6.1: Two Cells Scanned by Laser Beam

PC-Eye1 Fall Time



PC-Eye1 Rise Time

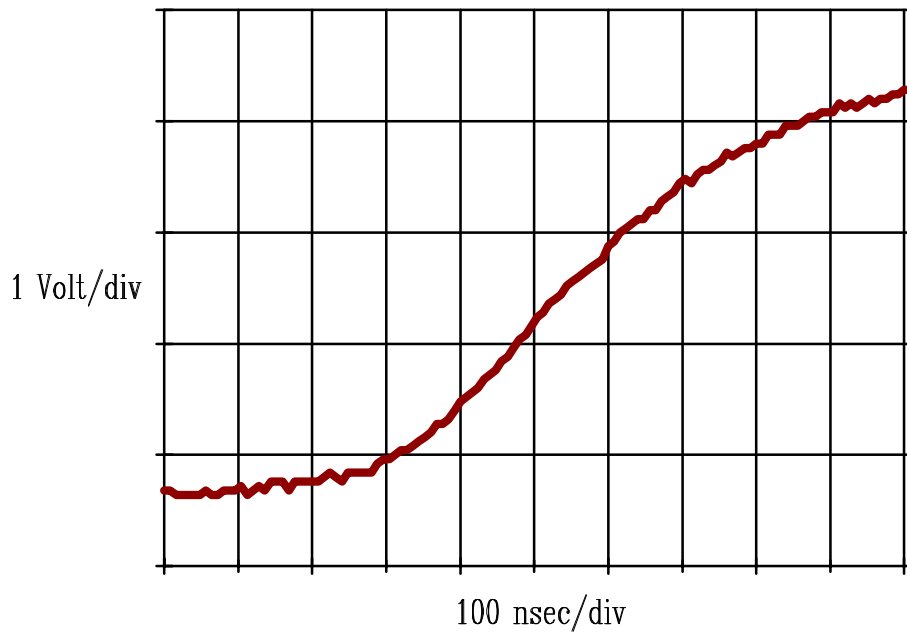


Figure 6.2: Response with Bar Code Scanner

7

Array Behavior

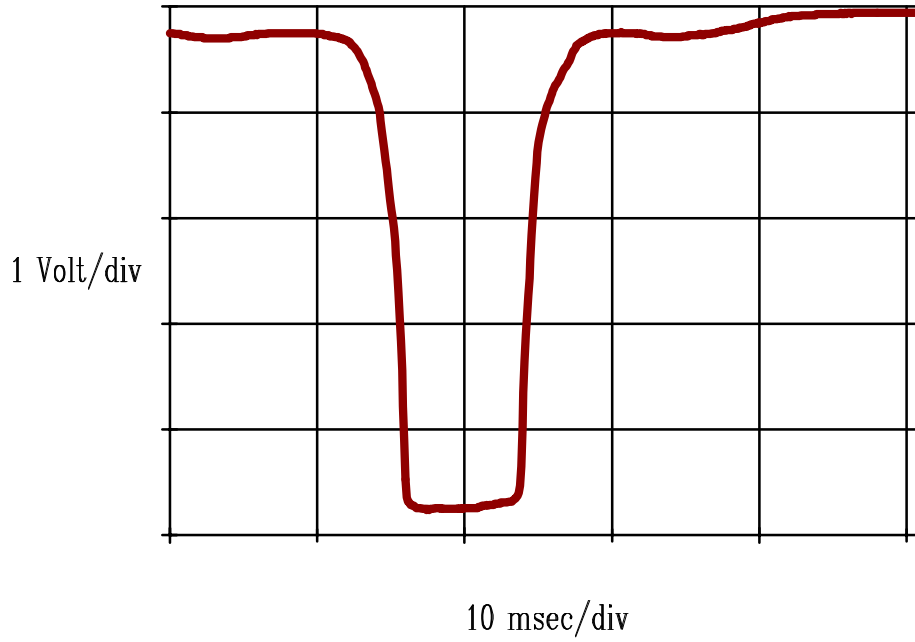
7.1: Setup

The array behavior of the Retina chip was measured with a multichannel ADC card installed in an IBM compatible PC. The Fluke 97 scope is not suitable for this experiment as it has only two input channels. The ADC card was programmed to sample output response from eight photocells in one of the four columns on the Retina chip. The eight cells chosen for this experiment had external connections at pins 18,19,20,21,22,23,24 and 26. Their relative positions are shown in appendix A. One pull-up resistor of 10k ohms was connected from each of these cells to dc supply of 5 volts. The supply voltage was kept to this value because that was the maximum permissible voltage for the ADC card. The ADC card monitored the voltage of these eight cells as a laser beam was scanned over the chip. To attain controlled scanning of the retina chip, the laser source C described in section 3.3 was used for this experiment.

7.2: Results

The lower trace in Figure 7.1 shows the response of eight channels superimposed when the chip is scanned by the laser beam. The upper trace shows the response of only one of these eight channels. The figure indicates good potential of the chip as an edge detector. Earlier experiments on the retina chip with conventional sources of light could not provide the level of resolution [7] achieved here with a laser beam.

PC-Eye1 Single Cell Response



PC-Eye1 Array Response

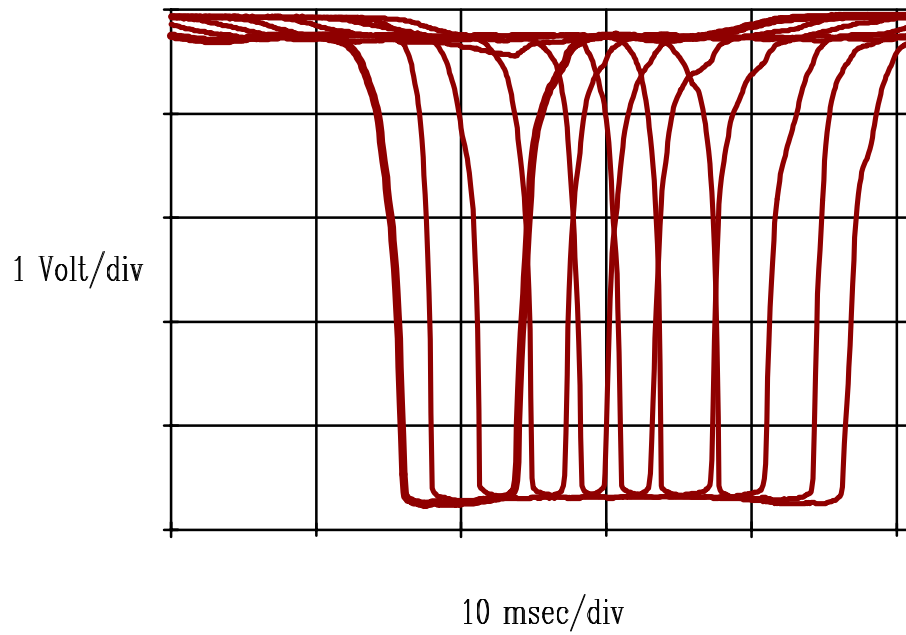


Figure 7.1: PC-Eye1 Array Response

8

Temperature Effect

To ascertain the temperature effects on the Retina chip, the forward voltage drop at pin 1 was measured at several temperatures, keeping the current flow fixed at 75 micro amps. The test module containing the chip was kept in the freezer compartment of a refrigerator. The test leads and power supply lines were brought outside for monitoring. The result is plotted in figure 8.1. The graph shows linear dependence of voltage drop on temperature. There is no surprise here, as this linear behavior is typical for semiconductor devices.

Forward Drop

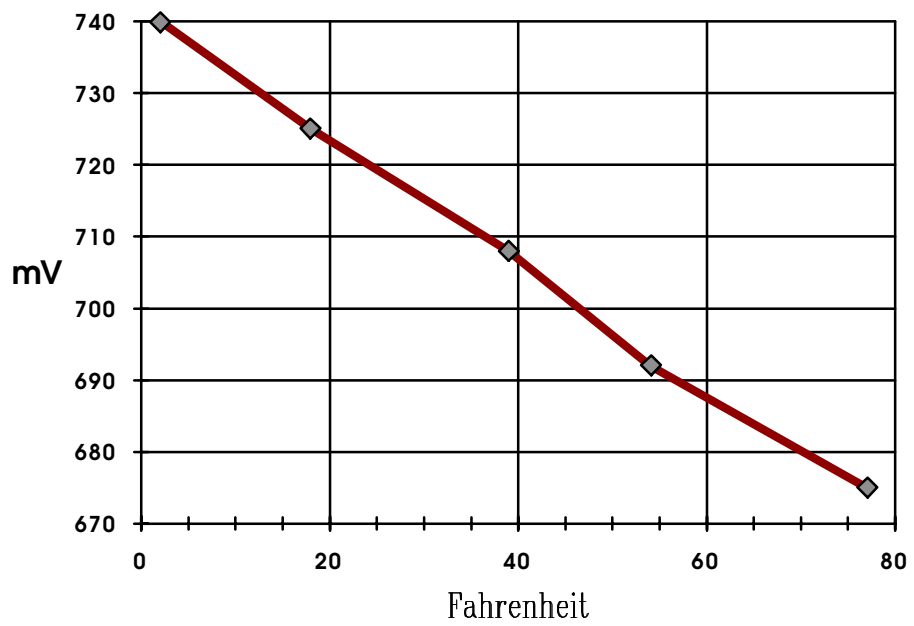


Figure 8.1: Forward Drop of Pin 1 at 75 micro amps

9

Beam Pattern

9.1: Setup

Several measurements were performed to estimate the spread of the laser beam. The Retina chip was mounted on a microscope translation stage. The laser source C described in section 3.3, was used for this experiment. It was preferred to the other sources because its focusing adjustments were done simply by a potentiometer. The Retina chip was mounted on a microscope, such that the chip is directly exposed to the beam. The microscope had precision translation stages so that the chip may be moved very precisely, scanning the laser beam. The laser source itself was not moved for this experiment. Pin 21 of the chip was chosen to monitor the beam intensity. This pin is internally connected to one of the small single cells, as shown in appendix A. One 270 ohms load resistor was connected from this pin to dc supply of 7.5 volts. The load resistor was kept much smaller than in other experiments to avoid saturating the photo-cell. In this laser source, there was a focusing lens integral with the laser head. The distance from the actual point of emission to the lens could not be measured, but the distance from the exterior edge of the lens to the chip was measured and reported in the following section.

9.2: Results

The voltage output across the load resistor and the corresponding translation stage positions of the microscope are plotted in Figures 9.1 through 9.4. It was observed that the sharpest possible image spot was formed when the focusing lens was extended as far out as possible. This gave the image position at about 500 microns ahead of the exterior edge of the lens. Keeping this distance from the chip, the microscope translation stage was moved laterally to measure the beam intensity in terms of the output voltage. The distribution is plotted in figure 9.1. The effective beam width was about a micron or less in this case.

On the other hand, the image spot was relatively enlarged, when the focusing lens was retracted as far in as possible. In this case, the image spot was formed at about 3000 microns from the exterior edge of the lens. As shown by Figure 9.2, the spread was more than one micron. As explained earlier, the actual distance from the point of emission to the lens could not be measured.

The effects of out of focus conditions are shown in Figures 9.3 and 9.4. Here the lens is kept in the same position as for the Figure 9.2 but the chip is moved out by a short distance away from the lens to create out of focus condition. With about 300 microns of longitudinal shift, the beam pattern becomes as shown in Figure 9.3. With about 1300 microns shift, the pattern

is further flattened, as shown in Figure 9.4. Here the effective beam width is approaching a millimeter.

Beam Spread

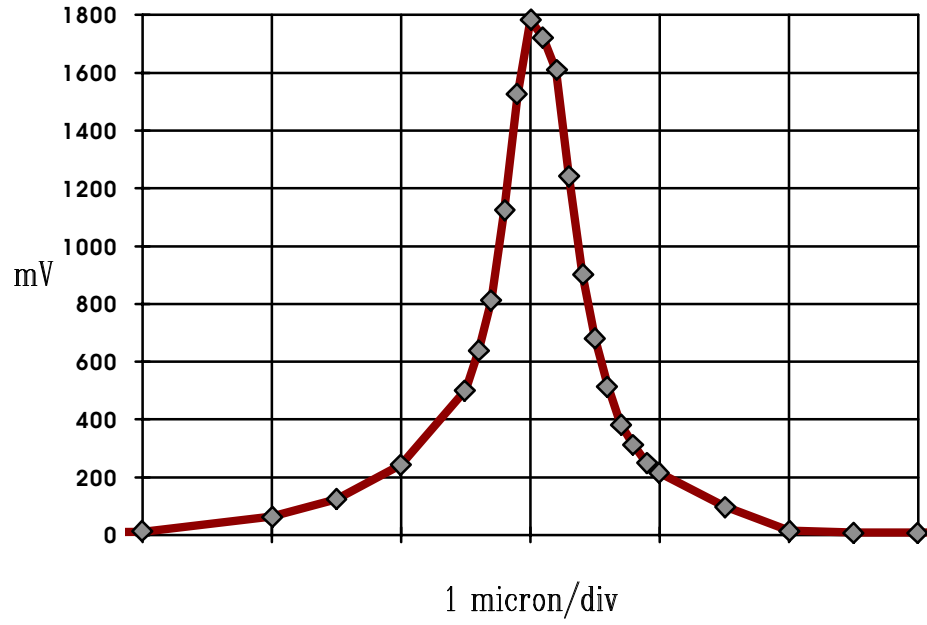


Figure 9.1: Beam distribution when focused at 500 microns from lens

Beam Spread

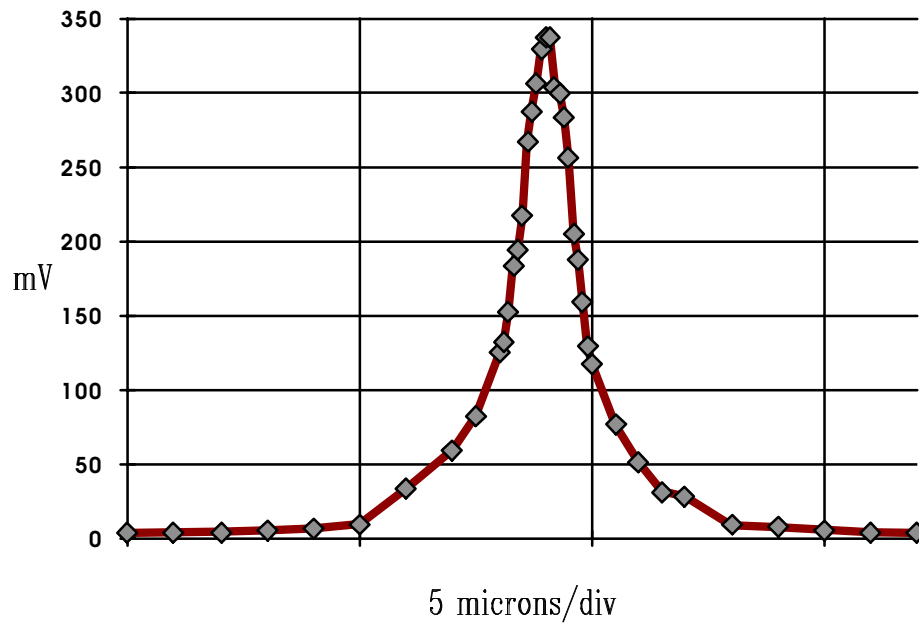


Figure 9.2: Beam distribution when focused at 3 mm from lens

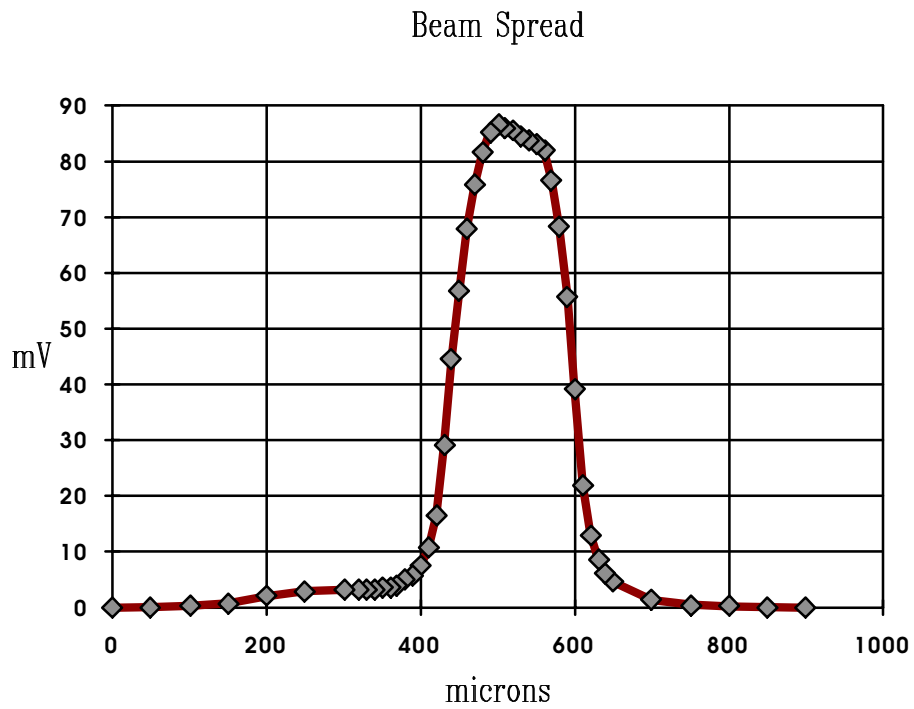


Figure 9.3: Slight out-of-focus condition from Fig.9.2

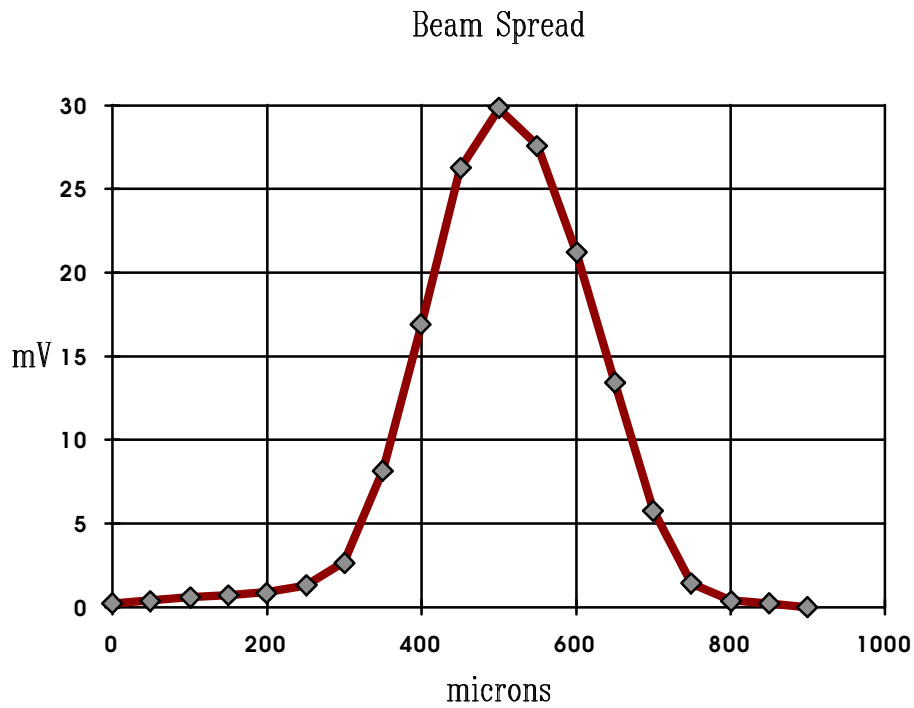


Figure 9.4: Large out-of-focus condition from figure 9.2

Edge Detection

The final goal of this investigation was to construct an edge detection circuit using the LLA Retina. A fuzzy edge sensor was reported by Mills [6], where he showed that negated implication is equivalent to a directed derivative, and that this property has the desired edge detection ability. For this experiment a LL9a chip was used to compute the implications. This device has 32 inputs and can be programmed to compute a wide variety of functions. The actual algorithm used for this experiment is shown in Figure 10.1. The actual circuit details and theory of operation are given in the following sections. The algorithm needed two continuous valued logic inputs from the photo cell clusters to the LLA. However each of these inputs was needed at two pins, simultaneously. This problem was resolved satisfactorily by using output from two adjacent cells in PC-Eye1, instead of direct copies. If the future LLA's have multiple fanout, then this problem can be resolved in the LLA itself, eliminating the need for external current mirrors or approximating substitutions.

The performance of the circuit is shown in Figure 10.2. The laser source C described in section 3.3, was scanned over the LLA Retina. When no edge was projected on the photo array, the output stayed low, but as the chip detected an edge, the output went towards a high level. The two peaks in the

figure resulted from the two edges at the entry and exit boundary of the beam that scanned the sensor.

10.1 Circuit Details

Here is the details of the edge detector circuit with LL9a and PC-Eye1 Chips:

Join Gnd to PC-Eye1 Pins 10, 25 and 35.

Join Gnd to LL9a Pins 10, 25, and 35.

Join Vdd to LL9a Pins 5, 15 and 30.

Join LL9a Pin 21 to PC-Eye1 Pin 32. This is one β signal referred later.

Join LL9a Pin 22 to PC-Eye1 Pin 9. This is one α signal referred later.

Join LL9a Pin 26 to PC-Eye1 Pin 33. This is another β signal referred later.

Join LL9a Pin 27 to PC-Eye1 Pin 8. This is another α signal referred later.

Join LL9a Pins 11, 20, 23, 28, and 31 to Gnd, with 47k ohms resistors.

Join LL9a Pin 40 to Vdd with a 47k ohms resistor. Measure output here.

10.2 Theory of Operation

Here is a detailed explanation of how the circuit works in theory. Assign symbol α for PC-Eye1 output at Pins 8 and 9, assume they are nearly same. Assign symbol β for PC-Eye1 output at Pins 32 and 33, assume they are nearly same. These two groups have similar sensitivity but are physically separated. According to the circuit, LL9a gets fuzzy logic ' α ' at 14-Alpha and 15-Beta. At the same time, LL9a gets fuzzy logic ' β ' at 14-Beta and 15-Alpha. The LL9a gets fuzzy logic '1' at 8-Beta, 13-Beta, 16-Alpha and 12-Beta. The LL9a gets fuzzy logic '0' at the remaining inputs. The resulting fuzzy expression for the output at Pin 40 involves five level implications involving all 32 fuzzy logic inputs. As reported by Mills and Daffinger [1] the LL9a will compute the following expression.

$$(((\mathbf{F} \rightarrow \mathbf{F}) \rightarrow (\mathbf{F} \rightarrow \mathbf{F})) \rightarrow ((\mathbf{F} \rightarrow \mathbf{F}) \rightarrow (\mathbf{F} \rightarrow \mathbf{T}))) \rightarrow (((\mathbf{F} \rightarrow \mathbf{T}) \rightarrow (\alpha \rightarrow \beta)) \rightarrow ((\beta \rightarrow \alpha)(\mathbf{T} \rightarrow \mathbf{F})))$$

This expression may be simplified as

$$(((\mathbf{F} \rightarrow \mathbf{T}) \rightarrow (\alpha \rightarrow \beta)) \rightarrow ((\beta \rightarrow \alpha)(\mathbf{T} \rightarrow \mathbf{F})))$$

After further simplification we get

$$(\alpha \rightarrow \beta) \rightarrow \neg(\beta \rightarrow \alpha)$$

This expression goes to false when both α and β approach each other. When they are wide apart, the above expression becomes true. Hence we have effectively incorporated edge detecting behavior from a real world point of view. This concept was originally given to this author by Professor Mills.

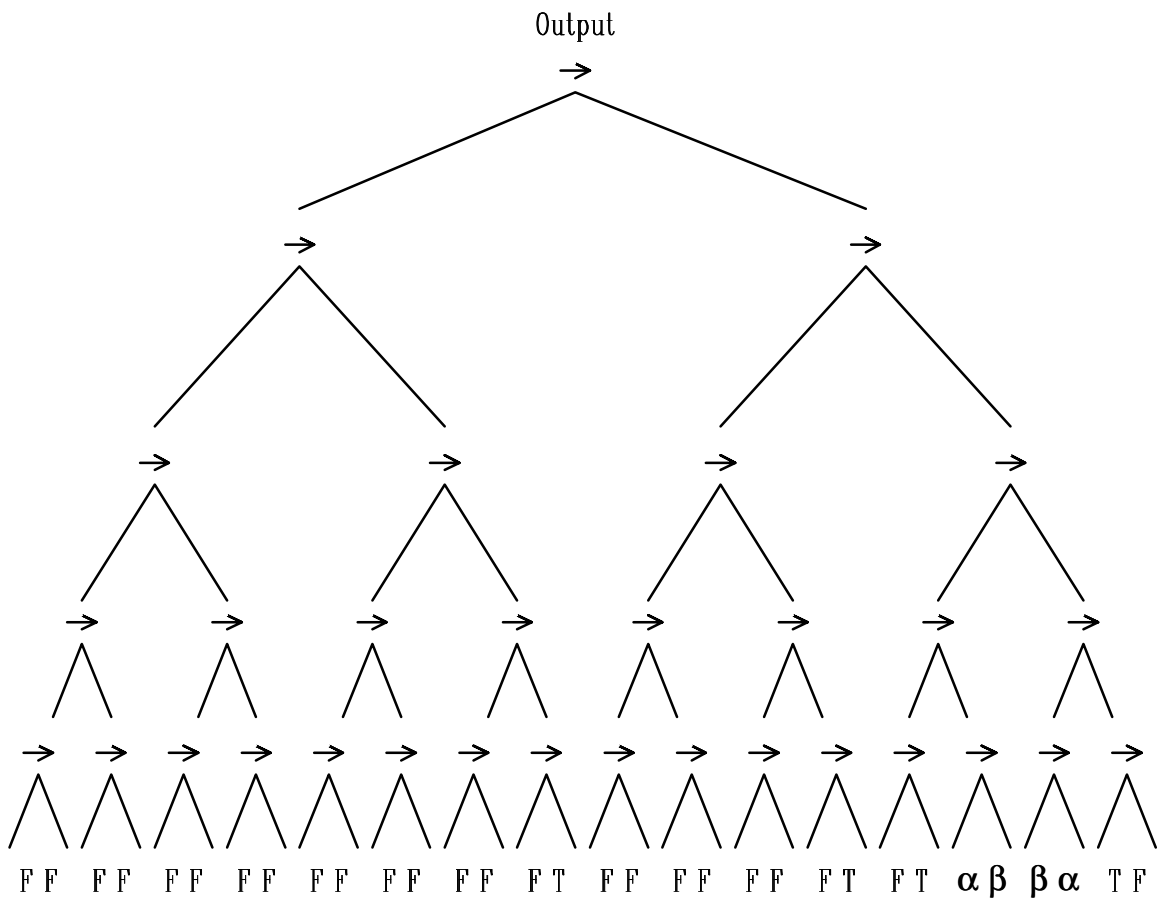


Figure 10.1: Logic Tree of Edge Detector using LLA9a

Edge Detection

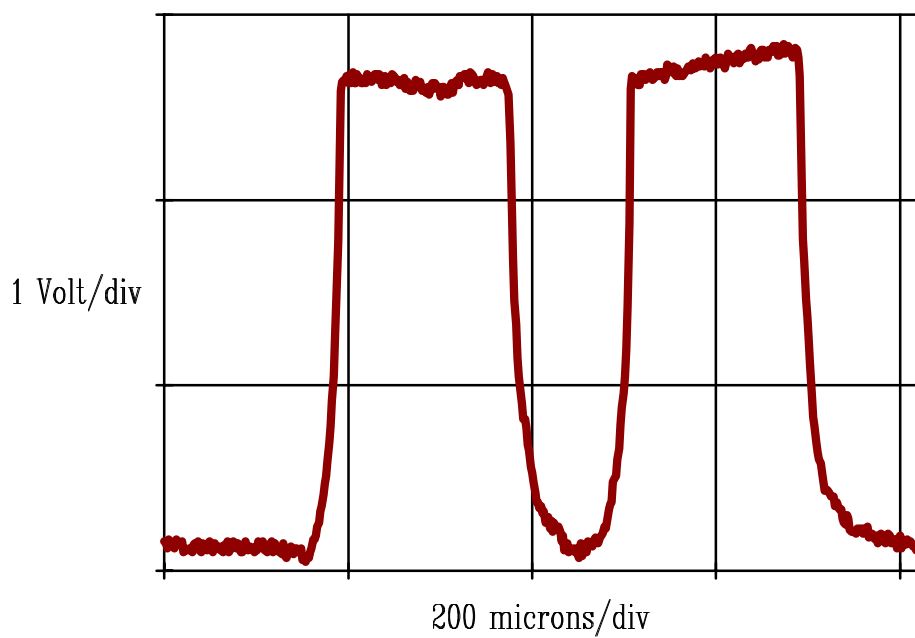


Figure 10.2: Edge Detection using LLA-Retina

Conclusions

A series of investigations was carried out on the LLA Retina system to evaluate its capabilities. For the current need of the robotics laboratory the sensitivity, resolution and speed of response of this system appear to be quite adequate. An edge detection algorithm was designed and tested using this concept. The edge detection algorithm required multiple copies of a particular logic variable to be applied at several locations simultaneously. This was approximated by logic levels from adjacent cells. If future LLAs have multiple fanout then this approximation may not be necessary.

The investigation reported in this thesis is nevertheless exhaustive. It may be interesting and useful to find the variations among the cells for each of the four groups of cells in the chip. It may be necessary to find the confidence limit of the characteristics by repeated experiments over large number of sample chips. Higher precision equipment may be necessary to compare the characteristics with other commercial devices of similar performance. It is hoped that LLA-Retina research will find applications in many diverse fields. Some of the activities that may be worked upon in the near future are :

Real time image processing by LLA-Retina.

A motion-sensor using fuzzy logic LLA-Retina,

An auto-focus system using fuzzy logic LLA-Retina,

Using parallel arrays of Retina chips for higher resolution,

References

- [1] Mills, J.W., M.G. Beavers, and C.A. Daffinger. 1990. *Lukasiewicz Logic Arrays*. Proceedings of 20th International Symposium on Multiple Valued Logic.
- [2] Edmund Scientific Company. 1994. *Annual Reference Catalog for Optics*. Science and Education. Barrington, New Jersey.
- [3] Mills, J.W., and C. Daffinger. 1990. *CMOS VLSI Lukasiewicz Logic Arrays*. Proceedings of Application Specific Array Processors. Princeton, New Jersey.
- [4] Mills, J.W., and C. Daffinger. 1990. *An Analog VLSI Array Processor for Classical and Connectionist AI*. Proceedings of Application Specific Array Processors. Princeton, New Jersey.
- [5] Mead, C. 1989. *Analog VLSI and Neural Systems*. Edited by L. Conway

C. Seitz and C. Koch. VLSI System Series/Computation and Neural System Series. Reading, Massachusetts: Addison-Wesley.

- [6] Mills, J.W. 1992. Area-Efficient Implication Circuits for Very Dense Lukasiewicz Logic Arrays. Proceedings of the 22nd International Symposium on Multiple-Valued Logic. Sendai, Japan.
- [7] Mills, J.W., A. Biswas and A. Heining. March 7, 1993. *LLAs and Edge Detection*. VLSI Laboratory Report, Computer Science Department, Indiana University, Bloomington, Indiana.
- [8] William Vaughan. 1985. *Handbook of Optics*. Optical Society of America,
McGraw-Hill Book Company, New York.

A. PC-Eye1 Cell Arrangement

For complete details on the cell layout, the reader should consult the original magic files, available at the VLSI laboratory, computer science department, Indiana University. The basic arrangement of the photo cells are shown below. There are four rows of photo cells. Three rows have eight photo cells each, but one row has only six photo cells. To understand the cell positions, look at the chip from top, keep pin 1 at top left, pin 40 at top right, pin 20 at bottom left, and pin 21 at bottom right. Now the matrix of photo cells will appear as shown below under a microscope. For example, the photo cell at the top left corner of the matrix, is connected to the pin 4 for external circuits.

4	3	2	1	40	39	38	37
9	8	7	6	36	34	33	32
-	17	16	14	13	12	11	-
18	19	20	21	22	23	24	26

The first row has eight 146x146 lambda doublet cells. The second row has eight 146x146 lambda single cells. The third row has six 32 x 32 lambda doublet cells. The fourth row has eight 32 x 32 lambda single cells. One cell from each of these four groups, was chosen for measurement of the static characteristics. For the first group, the cell corresponding to pin 1, was

chosen. The other three cells for the second, third and fourth groups were the cells with connections to pins 6, 11 and 20 respectively.

B. LL9a Pin Connections

Pin Number	Function	Pin Number	Function
1	2-Beta	40	Output
2	2-Alpha	39	10-Beta
3	1-Beta	38	10-Alpha
4	1-Alpha	37	9-Beta
5	Vdd	36	9-Alpha
6	3-Alpha	35	Gnd
7	3-Beta	34	11-Alpha
8	4-Alpha	33	11-Beta
9	4-Beta	32	12-Alpha
10	Gnd	31	12-Beta
11	8-Beta	30	Vdd
12	8-Alpha	29	16-Beta
13	7-Beta	28	16-Alpha
14	7-Alpha	27	15-Beta
15	Vdd	26	15-Alpha
16	5-Alpha	25	Gnd
17	5-Beta	24	13-Alpha
18	6-Alpha	23	13-Beta
19	6-Beta	22	14-Alpha
20	I-Ref	21	14-Beta

```

10 'data acquisition program
20 DIM DLO%(700, 8), DHI%(700, 8)
30 INPUT "enter file name ", F$
40 OPEN F$ FOR OUTPUT AS #1
50 BEEP: PRINT "grabbing"
60 FOR I = 1 TO 200: NEXT I
70 FOR X% = 0 TO 639
80 FOR I% = 0 TO 7
90 OUT &H220, I%: REM i% has channel number
100 A% = 0
110 A% = INP(&H220)
120 IF A% < 128 THEN GOTO 110
130 DHI%(X%, I%) = INP(&H221): REM read high byte
140 DLO%(X%, I%) = INP(&H221): REM read low byte
150 NEXT I%: NEXT X%
160 FOR X% = 0 TO 639:FOR I% = 0 TO 7
170 D=(DHI%(X%,I%)*16+DLO%(X%,I%)/16)*5/2048-5;" ";
180 PRINT #1,D;" ";
190 NEXT I%:PRINT #1,
200 NEXT X%
210 CLOSE
220 END

```

Table C.1: Typical Data Acquisition Program for the ADC card

```

10 'Data Transfer Program from Fluke97 to IBM-PC
20 'Requires Optical Interface from Fluke97 to PC
30 DIM A$(11000)
40 OPEN "com1:9600,n,8,1,rs,cs,ds,cd" AS #1
50 FOR I=1 TO 10000:J=0
60 IF EOF(1) THEN 80
70 A$(I)=INPUT$(LOC(1),1):NEXT I
80 IF I = 1 THEN 60
90 J=J+1:IF J<1000 THEN 60
100 PRINT,"done",I
110 INPUT "file name",F$
120 OPEN F$ FOR OUTPUT AS #2
130 FOR J=1 TO I
140 PRINT#2,A$(J);:NEXT J
150 PRINT,"over"
160 CLOSE:END

```

Table C.2: Typical Data Transfer Program from Fluke97 to Computer

&k0s0G ScopeMeter 97														
WAVEFORM Channel A 2.00mV/dot 80.0us/dot Y-pos 56dot														
54	55	54	56	56	54	56	55	53	56	56	56	56	55	57
54	56	54	54	54	55	56	57	54	54					
57	56	56	55	54	57	55	55	55	56	57	54	56	56	57
56	56	55	57	55	55	55	56	55	54					
55	55	54	56	54	56	57	54	56	54	54	55	55	56	56
55	53	55	55	54	54	55	56	57	54					
54	56	57	57	59	65	68	68	72	73	76	75	78	82	85
85	86	84	85	81	81	81	79	78	76					
77	75	73	73	71	72	69	69	69	68	68	67	68	66	66
63	64	64	63	62	61	60	62	60	60					
60	61	60	61	60	58	59	60	58	59	65	58	59	57	58
57	57	57	57	57	57	57	57	57	57					
55	57	57	57	57	57	56	57	55	56	57	57	56	57	56
57	57	57	56	58	57	57	57	53	54					
57	57	56	56	57	55	57	57	55	57	52	55	55	55	56
55	55	55	55	55	56	55	56	54	54					
55	56	55	55	55	57	54	56	55	56	56	55	56	56	55
56	57	56	54	55	55	56	55	55	55					
55	54	57	56	55	57	56	56	55	54	55	55	55	57	56
56	56	56	57	57	56	55	55	55	56					
55	55	56	57	55	55									

Table C.3: Typical Data Dump from Fluke97 to Computer

Units and Conversions

Table D.1: Units of Luminous Flux Density at a Surface:

SI and mks unit	lux	(lx)	lumens per square meter
cgs unit	phot	(ph)	lumens per square centimeter
English unit	foot-candle	(fc)	lumens per square foot

Table D.2: Conversion of Illuminance Units(ANSI Z7.1-1967)

	foot-candle	lux	phot
1 foot-candle	1	10.76	0.00108
1 lux	0.0929	1	0.0001
1 phot	929	10000	1

Table D.3: Typical Light Sources

He-Ne Laser Tube	1 milliwatt
Infra-red/visible Laser Diode	1 milliwatt
40 watt soft white bulb	490 lumens
52 watt miser plus bulb	700 lumens
650 watt photo flood bulb	20000 lumens
Solar radiation (approx. 6000 K)	135 mw/sq.-cm

Figure E.1: Photograph of PC-Eye1 on Test Board

Figure E.2: Photograph of Responses at Pin 21 and Pin 26

Curriculum Vitae

Amitava Biswas was born on September 4, 1950, in Calcutta, India. In 1971, he obtained a Bachelor of Technology (Honors) degree in Mechanical Engineering from Indian Institute of Technology, Kharagpur, India. He was Assistant Professor of Mechanical Engineering at the same Institute from 1985 to 1990. He came to Bloomington in the fall of 1990, to attend the graduate program of Indiana University's Computer Science Department.

